IEEE Access
Multidisciplinary | Rapid Review | Open Access Journal

Received April 26, 2020, accepted May 8, 2020, date of publication May 14, 2020, date of current version May 28, 2020.

Digital Object Identifier 10.1109/ACCESS.2020.2994382

Fully Planar Dual-Polarized Broadband Antenna for 3G, 4G and Sub 6-GHz 5G Base Stations

SERGIO MARTIN-ANTON AND DANIEL SEGOVIA-VARGAS, (Member, IEEE)
Group of Radiofrequency, Electromagnetics, Microwaves and Antennas (GREMA), Signal Theory and Communications Department, Universidad Carlos III de Madrid, 28911 Madrid, Spain

Corresponding author: Sergio Martin-Anton (sergmart@ing.uc3m.es)

This work was supported in part by the Spanish Ministry of Education, Culture and Sport under a grant for predoctoral contracts for University Teacher Training under Grant FPU16/00459, and in part by the Spanish Ministry of Science, Innovation and Universities, (program "Programa Estatal de I+D+i orientada a los Retos de la Sociedad") under Grant RTC-2017-6394-7.

ABSTRACT A fully planar dual polarized radiating element with internal embedded coupled dipoles is presented in this paper. The inclusion of these elements allows achieving three different goals: firstly, an extension of the bandwidth towards lower frequencies (from 1.69 GHz to 1.427 GHz) as required in new 5G standards; secondly, a reduction of the antenna size in comparison with other topologies for bandwidth extension and, finally, a reduction of the secondary lobes. The proposed dual polarized broadband antenna is based on two sets of dual polarized dipoles, with a fully planar structure. The objective of this paper is the design of an antenna working in the extended 5G band in order to fulfil the future 5G requirement in the microwave region, in which the new frequency bandwidth goes from 1.427 up to 2.69 GHz with the return losses lower than −14 dB and the crosspolar isolation larger than 28 dB.

INDEX TERMS 5G, base station, broadband antennas, dipole, dual polarization, mobile communication, planar antennas.

I. INTRODUCTION

Nowadays, the new challenges in the communication systems such as the biggest number of connected devices ever known with an extremely low latency and highest data rates ever used has brought the arrival of new 5G systems. These demands imply that users will require higher bandwidths for mobile connections. In addition, the explosion of connected devices as in the new IoT (Internet of Things) technology makes that more than 20 billions of connected devices will be available in 2020 [1]. The challenge to satisfy the new technological demands implies huge efforts to increase the bandwidth and obtain high bit rates (i.e. 10 Gbits/s or higher).

New mobile communication services have to use new strategies for optimizing current spectrum resources and achieve the required higher data rates [2], [3]. Among these techniques it can be mentioned an increase towards higher frequency bands such as millimeter bands or the application of new advanced modulation techniques such as carrier aggregation (CA). It is also important to highlight the coexistence of future 5G networks with the actual 3G and 4G standards.

The associate editor coordinating the review of this manuscript and approving it for publication was Shah Nawaz Burokur.

In a recent releasable report [4] it is stated that 5G new radio (NR) gives a unified and more capable air interface providing diversity in three aspects: diversity in services (from critical services to massive Internet of Things –IoT- ones and enhancement of current mobile services), diversity in deployments and, finally, diversity in spectrum. This spectrum diversity for 5G NR provides a division in the frequency spectrum in three regions: low bands (below 1 GHz), mid-bands (between 1 and 6 GHz), and high bands (above 24 GHz). The first two bands (low and mid) constitute what it is currently known as sub-6 GHz bands. This paper focuses on the mid sub-6 GHz band. Previously, in Table 2 in [5], a survey on 5G technologies broadly uses the terminology "5G sub-6 GHz" to refer to widely distributed spectrum from 450 MHz up to 6 GHz. That classification comes from [5] where the operating bands for standalone services with carrier aggregation (CA) or dual connectivity (DC) were proposed. In particular the bandwidth between 1427 MHz up to 2690 MHz is one of the proposed for NR-DC services. Therefore, the international administrations have allocated part of the L-band (1427-1518 MHz) to provide additional bandwidth for mobile communications. In particular, the standardizing of 5G [6] allows the bandwidth from 1427 MHz for NR-UE (user equipment). In addition,

the European Union [7], [8], has included the harmonization of part of the L-band (1427 MHz to 1518 MHz) for the next-generation (5G) terrestrial wireless systems.

From the technological point of view the associated mid-band for 3G and 4G services (between 1710 and 2690 MHz) has to be extended down to 1427 MHz resulting in a new extended band from 1427 MHz to 2690 MHz. In addition to the bandwidth extension, a reduction in size would also be welcome due to environmental issues. Then, for these new antennas, not only does the frequency band need to be extended but also the antenna size has to be reduced while keeping suitable performance in its radiation pattern and matching and isolation parameters.

In the last years, different broadband antennas for base stations have been developed. Patch and dipole-based antennas, such as crossed bow-tie dipoles, have been extensively used for base-station antennas. Whereas patch antennas are good because of their compactness its performance when requested to work in bandwidths larger than 50% is more complicated. In fact they need the addition of parasitic elements or stacked structures to get the required bandwidth. So, as seen in the literature, crossed dipoles, folded dipoles, bow-ties, and in general dipole-based antennas have been a more common choice for this wide band performance. However, in general, the operating bandwidth of those antennas does not cover the desired extended band. Then, in [9], [10] a pair of printed dipoles was proposed to achieve a slightly extended bandwidth (1.65-2.85 GHz) for LTE applications but for a general single polarization case. Eventually, a double element for dual polarization on a 130 × 130 mm2 cell was proposed but leading to a much larger and asymmetric structure with tilted patterns.

In [11]–[16] different kinds of crossed bow-tie dipoles were presented to cover the non-extended band from 1.7-2.7 GHz. None of the previous works deal with the challenge of the extended bandwidth. In [17] a reduction of the antenna size was shown by using folded dipoles at a price of covering even a shorter bandwidth than the one for 2G-3G applications. In fact, although the dimensions of the antenna were certainly small, the antenna only covered the bandwidth between 1.7 and 2.25 GHz (far away from the required needs for the extended 1.427 GHz to 2.7 GHz).

Different attempts have been made to achieve compact designs. In [18] the use of multi-resonant cross-dipoles allowed obtaining compact antennas but without either covering the new extended bandwidth. The use of Artificial Magnetic Conductors (AMC) in [19], [20] helped to reduce the height of the antennas but with higher values of the return losses (values around −10 dB instead of −14 dB) and, also, without covering the extended bandwidth.

It has not been till very recently that the proposed extended band has been included in the radiating elements for the newest base stations. The challenge is great since a coexistence with the previous 3G and 4G communication systems has to be achieved. One attempt aiming to reduce the size, while covering part of the mid-band sub-6GHz 5G bands (between 1.7 and 3 GHz), can be seen in [21]. However, the lowest part of the extended band is not covered and its inclusion in array topology is not straightforward since the antenna is not planar. In [22] an example using crossed bow-tie dipoles is presented but the need of a conformal shape reflector yields to larger dimensions. Finally, two topologies have been presented in [23] where the inclusion of parasitic elements allows enhancing the bandwidth of previous bow-ties or dual dipoles. In that work, the inclusion of stacked parasitic capacitor made possible to add a new resonance in the higher band but at the price of having a multilayer non-compact design, what makes mass fabrication more difficult.

TABLE 1. BWs and sizes of broadband base station antennas.

Ref.	BW (GHz) (%)	Element Size (mm) (λ_L)	Isolation(dB)
[12]	1.71-2.71 (45%)	67.2x67.2x29 0.38x0.38x0.16	30
[13]	1.7-2.7 (45%)	68.2x68.2x32 0.39x0.39x0.18	26
[14]	1.69-2.71 (45%)	70.38x70.38x27 0.4x0.4x0.15	28
[16]	1.61-2.71 (51%)	70.4x70.4x42 0.38x0.38x0.23	30
[17]	1.7-2.25 (28%)	80x80x34 0.45x0.45x19	25
[18].1	1.7-2.69 (45%)	46.7x46.7x32 0.27x0.27x0.1	35
[18].2	1.65-3.3 (66%)	52.2x52.2x34 0.44x0.44x0.26	28
[19]	1.7-2.7 (45%)	70x70x18 0.4x0.4x0.1	25
[21]	1.7-3 (55%)	150x150x100 0.35x0.35x0.23	20
[22]	1.427-2.9 (68%)	134x110x33 0.63x0.52x0.16	20
[23].1	1.4-2.7 (64%)	132.8x132.8x45.3 0.62x0.62x0.22	30
[23].2	1.4-2.7 (64%)	80x80x55.8 0.37x0.37x0.26	30
Present	1.4-2.7 (64%)	77x77x45 0.36x0.36x0.13	30

This work presents a compact and fully planar antenna for 3G-4G and sub 6-GHz 5G for large coverage area base stations. This challenge has been dealt by jointly acting on the radiating element and on the feeding structure. Concerning the radiating element, the inclusion of internal dipoles simultaneously coupled and fed by the feeding line and through the main dipoles allows extending the frequency band while keeping a compact and fully planar structure. In addition, the compactness of the new antenna prevents the multilobe effect at higher frequencies. Finally, concerning the feeding structure, the transition between the coaxial probe to the microstrip one has allowed achieving a nearly symmetric dual polarized broadband structure. Table 1 shows a comparison

of the referenced dual-polarized broadband antennas and the presented in this work. For a fair comparison the size of any antenna is normalized in terms of λL (where λL is the wavelength at the lowest working frequency). The proposed antenna consists a fully planar one and shows the smallest size among all the ones covering either the extended bandwidth or a bandwidth larger than 60%.

The paper is organized as follows. Section I gives the Introduction. Section II focuses on the radiating element. Section III deals with the feeding structure. Section IV provides the manufacturing issues and experimental results while Section V concludes the paper.

II. BROADBAND DUAL-POLARIZED COMPACT ANTENNA

A. NON-COMPACT DUAL-POLARIZED BROADBAND ANTENNA

The challenge in the development of new antennas for sub 6-GHz 5G applications raises a demand on a dual contradictory statement. On one side, smaller and smaller sizes are required, whereas on the other, larger and larger bandwidths are needed. It is well known that the antenna bandwidth is constrained by its electrical length [24]. Then, the extension to lower frequency bands, while keeping the largest ones and even reducing the size of the radiating element, is a challenge itself.

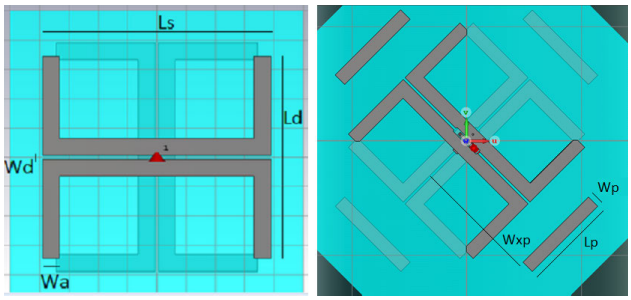

FIGURE 1. Schematic of the proposed antennas: the left part shows the non-extended bandwidth whereas the right one shows the extended bandwidth non-compact antenna.

An arrangement of a double set of dual dipoles was used in [25] to achieve a dual-polarized configuration. The antenna, illustrated in Fig. 1, is composed of a pair of two dual dipoles connected in parallel through a coplanar strip on each side of the substrate. This dual polarized element (left part of Fig. 1) presents two resonances: one associated to the length of the dipole itself and the other associated to the extended dipole coupled to the backside dipole. The feeding of the antenna consists of a microstrip bridge that balances one of the coaxial conductors to connect it to one dipole branch through the substrate. For the first polarization the H-shaped dual dipoles are printed on the substrate backside whereas the microstrip bridge is on the front side. For the second polarization the process is just in the opposite sense. The addition of external strips (right part of Fig. 1), acting as capacitive parasitic elements, enhances both the return losses and their associated bandwidth. The objective of placing these parasitic elements is to get another resonance that fulfills the bandwidth requirements. Including parasitic elements enhances the matching and bandwidth but also increases the size of the antenna. The antenna is designed on a Roger 4350B substrate, with a relative dielectric constant of $\varepsilon = 3.48$ and a thickness of $h = 0.76\ mm$. The proposed broadband antenna has to cover the extended frequency bandwidth between 1.427 and 2.69 GHz while maintaining original base station specifications such as $VSWR$<1.5, $isolation$<$-28dB$ and $beamwidth = 65° \pm 10$.

The realization of the current antenna requires a flat ground plane reflector placed 45 mm below the radiating element (corresponding to $\lambda/4$ at the central frequency). This assures the best matching condition while keeping a trade-off with the desired beamwidth. The dipoles length, $Ld = 68.8\ mm$, is chosen to select the intermediate resonance frequency. Concerning the coplanar strips, the width of the line will be the same as the one of the dipole ($Wa = 5.8mm$) whereas the spacing between the lines has been set to 1.2 mm (Wd). Finally, concerning the external parasitic strips, it can be said that are placed at both sides of the dual dipoles acting as side capacitive elements to improve the matching at higher frequencies and enlarge the overall bandwidth. The values for the parasitic elements were chosen to add a third resonance frequency around 2.6 GHz resulting in the following values: $Lp = 38.5mm$, $Wp = 6mm$, and the $Wxp = 87.5mm$ as can be seen in the right part of Fig. 1. A comparison of the impedance bandwidth between the antennas at the left and right part of Fig.1 is shown in Fig. 2. The proposed impedance bandwidth has been clearly achieved with the inclusion of these capacitive elements.

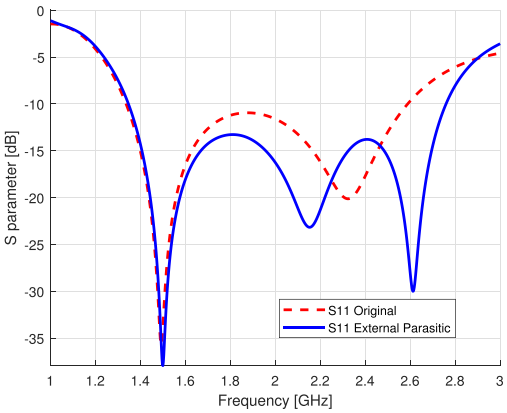

FIGURE 2. S_{11} Parameter for the proposed antennas (continuous line shows the extended frequency non compact antenna whereas the dashed line shows the non-extended frequency).

The inclusion of the parasitic element has allowed increasing the impedance bandwidth at a price of enlarging the electric dimensions of the antennas. This fact is particularly critical on the antenna radiation pattern that tends to have a multilobe performance at higher frequencies, when the dimension of the overall antenna is larger than λ. This can be seen in Fig. 3 that shows the horizontal plane of radiation

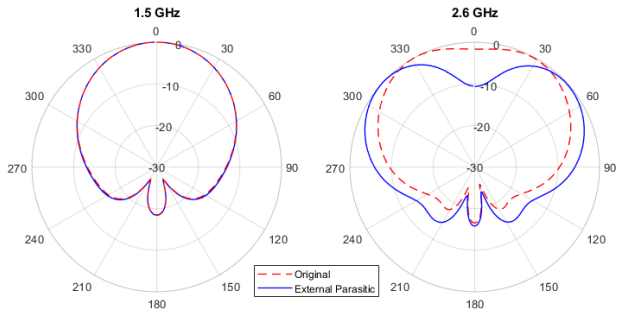

FIGURE 3. Radiation Pattern of External Parasitic Antenna present lobulation for highest part of frequency band (Discontinuous red line for original element, continuous blue line for external parasitic).

pattern for both antennas, non-extended and extended frequency antennas. A non-desired lobe appears in the extended frequency antenna due to its dimension, larger than a wavelength ($D > \lambda$).

B. EXTENDED BANDWIDTH DUAL-POLARIZED COMPACT ANTENNA

The inclusion of internal dipoles simultaneously coupled and fed by the feeding line and through the main dipoles allows extending the impedance bandwidth while keeping a compact and fully planar structure. In addition, the compactness of the new antenna prevents the multilobe effect at higher frequencies. The final goal is the reduction of the multilobes in the previous non-compact dual polarized broadband antenna.

Fig. 4 shows three possibilities to extend the bandwidth and reduce the antenna size. In all of them the total dimension of the antenna is smaller than the wavelength at the highest frequency in order to avoid multilobe radiation patterns as desired for the whole frequency band.

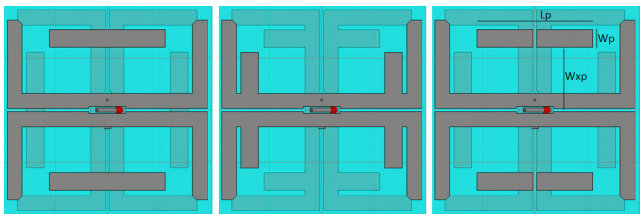

FIGURE 4. a) Internal Parasitic. b) Internal fed Dipoles. c) Internal Parasitic Dipoles.

The first option (shown in Fig. 4a) is the addition of a fully parasitic strip integrated inside the element in a similar way to the one proposed for the non-compact antenna (it is called as internal parasitic in Fig. 4a). These strips are intended to provide an additional resonance at the highest frequency band (in this case around 2.7 GHz). The strips have to be placed on the opposite side of the substrate in order to avoid physical contact with the original conductors. These continuous strips affect the feeding coplanar strips and perturb the original dipoles of the antenna and the matching of the element. Despite the similarity with the antenna of the previous section, the optimized parameters (the strip length, L_p, the strip width, W_p, and the separation with the main dipole, W_{xp}) do not turn out a good performance of the antenna in terms of impedance matching and sidelobes.

The second option consists on making the internal dipole active by feeding it through the line. This internal dipole is placed in ohmic contact with the coplanar strips generating a new resonance at higher frequencies. Although the impedance bandwidth is extended and the lobes have been reduced, there is an increase in the return losses at central frequencies that is not easily controlled.

By acting on the impedance and on the coupling of the added dipole (mostly by means of modifying both the width of the new internal dipole, W_p, and its position with respect to the main dipole, W_{xp}) a control on the overall impedance bandwidth, in particular at middle frequencies, can be achieved. However, due to physical limitations, the dipole has to be placed in antipodal configuration at the opposite side of the main dipole as shown in Fig. 4c. Then, the final arrangement of the proposed antenna is as follows. For the central frequency, 2.3 GHz, the dipole length approximately equals $\lambda/2$, generating a resonance for that frequency. This can be appreciated in the central part of Fig. 5. Another resonance is found at 1.5 GHz. This is due to the coupling between the original dipole and its antipodal part, as can be appreciated in the left part of Fig. 5. A current distribution along the dipole and its antipodal part flows along a length of 140 mm, what approximatly matches $\lambda/2$ at 1.5 GHz. Finally, as shown in the right part of Fig. 5, another resonance appears at 2.7 GHz associated to the coupled inner dipole in the antipodal part of the main dipole. The dimensions of all the design parameters of the antenna are shown in Table 2. This table also shows the distance with the ground plane, H_G, which has been set to 45 mm.

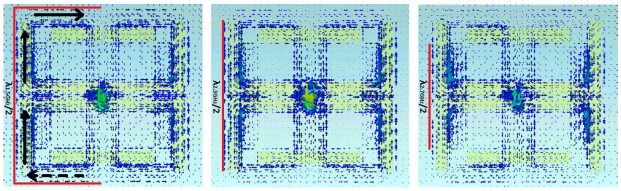

FIGURE 5. Currents for vertical excitation. 1.5, 2.3 and 2.7 GHz frequencies are presented.

TABLE 2. Parameters for new design with internal parasitic dipoles.

Parameter	Value [mm]
Wd	1.2
Ld	68.8
Ls	77
Wa	5.8
Lp	46.5
Wxp	25.25
Wp	6
H_G	45

Once the impedance bandwidth has been studied, two additional points have to be addressed concerning the radiation

pattern. The first one is associated to the presence or not of multilobes. According to the current distribution shown in Fig. 5 it can be seen that the inclusion of the new dipole has avoided the presence of multiple lobes in the current distribution and in the radiation pattern along the whole band.

The second point is the crosspolar radiation that could be high, at least at the lowest frequencies due to the coupling between the dipole and its corresponding antipodal part. Fortunately, this does not happen and the cross-polar component is low enough. This can be explained, for one polarization (the other one is equivalent), as follows. When the vertical dipoles are fed, the phase associated to its input port 1 (P1) is maximum while the one associated to port 2 (P2) is null. Under these conditions the currents in the extended vertical dipole (vertical dipole plus the coupled horizontal arms) are shown in Fig. 5a. These currents allow having an extended length for the dipole, what makes the working frequency be reduced for the radiation copolar component. However, for the crosspolar component the horizontal currents are cancelled out since the upper part of the current (a continuous trace has been added in the right part of Fig. 5) is 180° out of phase in comparison with the bottom one (dashed trace) producing a cancelation of the horizontal current contribution and a subsequent reduction of the crosspolar component.

The resulting S-parameters are shown in Fig. 6. The return losses are lower than −13 dB for both ports along all the frequency band, between 1.4 to 2.8 GHz (and lower than −15 dB for most band). In addition, the isolation is larger than 35 dB along the bandwidth between 1.4 and 2.6 GHz and larger than 30 dB in the whole extended band up to 2.8 GHz.

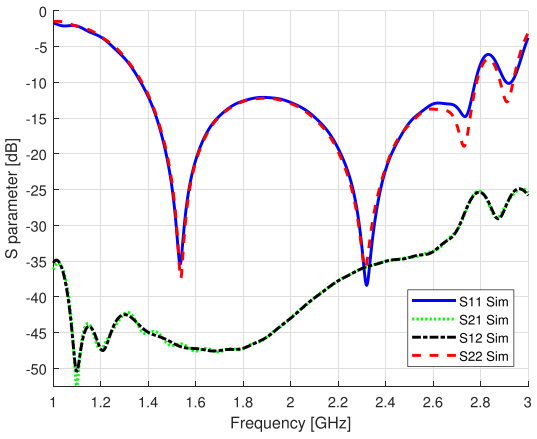

FIGURE 6. S parameters for internal parasitic dipoles antenna.

C. FEEDING

The final step for the design is the feeding network. This stage is critical, especially, because of the broadband performance of the structure and the balanced arrangement of the antenna itself. Then, a broadband balun to balance the coplanar feeding for the two pairs (horizontal and vertical) of dipoles with the unbalanced coaxial line is needed. Fig. 7 shows the overall structure of the balun. For the horizontal pair of dipoles the feeding will be made through the coaxial port 1. Its outer part

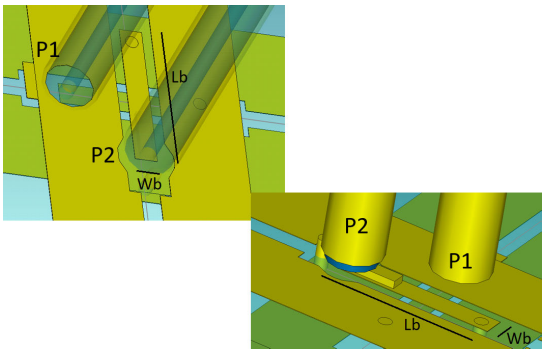

FIGURE 7. Coaxial feeding architecture. Picture shows both coaxial inner conductor connected to the bridge and the jacket to one dipole branch.

is directly welded to one branch of coplanar strips, whereas the inner conductor crosses the substrate through a hole. The double side cladding substrate allows creating a metal strip between the coplanar conductors of the vertical pair of dipoles placed on the other side of the substrate. This metal strip will serve to create a bridge with the horizontal dipoles via a hole and an ohmic contact. The described overall structure will act as a balun and will balance the signal from port 1 to the horizontal dipoles. The dimensions of this global microstrip bridge are important parameters for achieving the desired impedance matching along the desired broadband. The values of its width, W_b, and length, L_b are: $W_b = 1.4mm$ and $L_b = 9.3mm$. This procedure has to be repeated for the feeding structure through the coaxial probe P2 for the vertical polarized antenna as shown in Fig. 7.

Finally, a microstrip taper has also been included to match the impedance to 50 ohm. This transition will be placed on the other side of the ground plane and will improve the impedance matching to values below −15 dB between 1400 MHz and 2800 MHz. This can be appreciated in Fig. 8 that compares the impedance matching with the taper and without the taper.

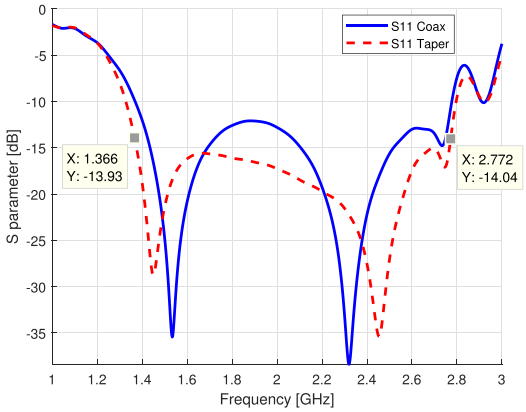

FIGURE 8. Return losses with and without taper feeding.

III. EXPERIMENTAL RESULTS

The antenna has been fabricated with a routing laser machine. The balun has been realized with two coaxial cables that connect the two branches of the dipole through a bridge with

dimensions L_b and W_b as described in Section II.C. A flat ground plane has been added since it is easier to fabricate than a conformal one and shows good performance for our application. The reflector also acts as a ground plane for the needed circuits, in particular for the proposed microstrip taper for the feeding. In addition some nylon posts have been added to provide mechanical robustness and assure the required distance between the antenna and the ground plane. It has been previously proved that the presence of the posts does not affect the electromagnetic properties of the antenna. This arrangement can be seen in Fig. 9 that shows the antenna to be measured in the anechoic chamber.

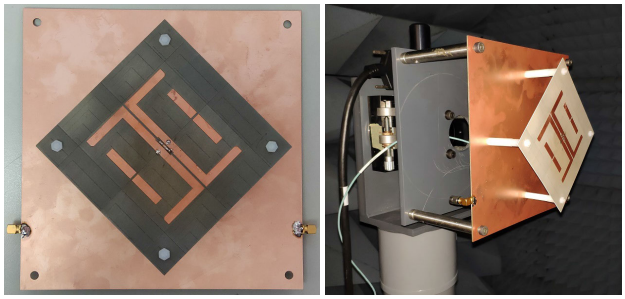

FIGURE 9. Pictures of the antenna prepared to be measured in the anechoic chamber.

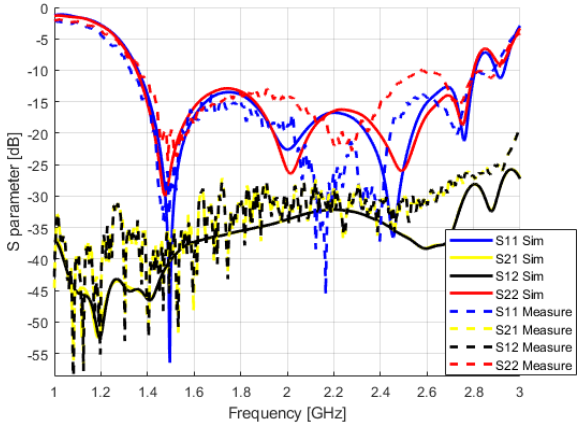

FIGURE 10. S parameters of the antenna. Simulated in continous line and measured in dash line.

Fig. 10 shows the S parameter of the final prototype for the presented antenna. Both the reflection coefficient and the isolation between ports are shown. A comparison between simulations and measurements has been undertaken. Good agreement between simulation and measurements can be seen in Fig. 10. The reflection coefficient at port 1, S_{11}, is below -14 dB, both in simulation and measurement for the whole frequency band, from 1.4 to 2.8 GHz. The same happens for the second port, S_{22}, except a small mismatching (but always below -10 dB) in the upper part of the band (between 2.5 and 2.7 GHz). This prominence between 2.5 and 2.7 GHz is probably due to the different and more laborious coaxial welding. Finally, the isolation between both polarizations fully meets the requirements around 30 dB for the whole

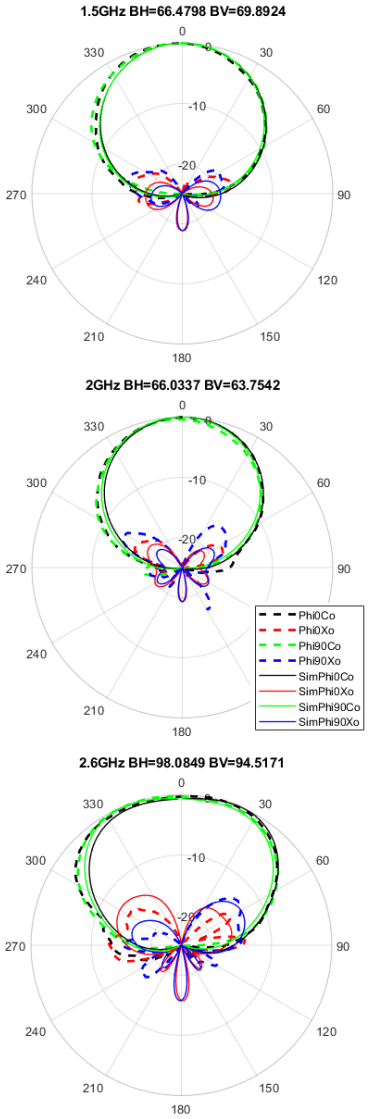

FIGURE 11. Simulated and measured radiation pattern.

frequency band achieving a value below -28 dB between 1.427 and 2.69 GHz.

Finally, with regards to the radiation pattern, it is well known that base stations usually have sector architecture what means that the different sectorial antennas are combined in one place to obtain the required omnidirectional diagram. When applied to one sector antenna, it means that the broadband design has to achieve a stable radiation pattern within the desired bandwidth for both polarizations with a horizontal radiation pattern around 65 degrees. Fig. 11 shows the radiation pattern at three frequencies (1.5 GHz, 2 GHz and 2.6 GHz) for both horizontal and vertical planes for copolar and crosspolar polarization ($\pm 45°$). As illustrated, there is a good agreement between simulations and measurements. The horizontal half-power beamwidth, as required, is very stable for most of the band with values of 66°. It can be appreciated, however, that wider beamwidths are found at higher frequencies. This increase can be due to the fact that

potential lobes are close to appear implying an increase in the corresponding beamwidth.

It can also be appreciated that the copolar-crosspolar ratio is larger than 25 dB are achieved for a beam range between ±30° for the whole frequency range (between 1.4 GHz and 2.7 GHz). For larger beamwidth ranges (up to ±90°) the copolar-crosspolar ratio is always larger than 15 dB. This is coherent with the fact that the feeding structure and the arrangement of the dipoles cancels out the currents orthogonal to the desired one, as it was explained in Section II.B. The same can be said for the vertical beamwidth, good agreement with the simulation can also be seen.

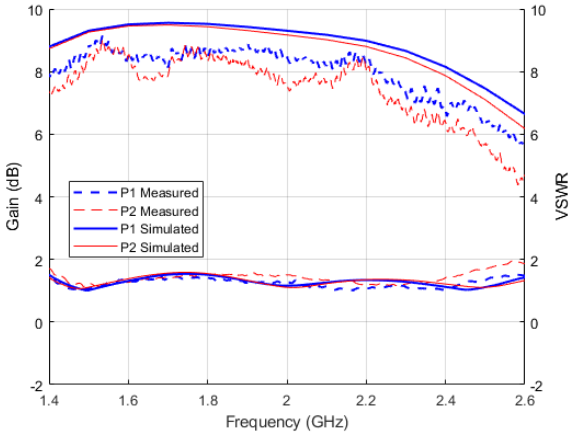

FIGURE 12. Antenna gain at boresight. Simulated and measured for both ports.

Finally Fig. 12 summarizes the values for the realized gain at boresight and the corresponding *VSWR* for the whole bandwidth. The gain in simulation shows values around 9 dBi whereas the measurement is around 8 dBi. This small difference can be due to some transition and connector losses. Finally, the small difference between port 1 and port 2 can be associated to the inequality between the feeding at port1 and 2, meaning that small differences observed in matching are also presented in the realized gain values. Concerning the *VSWR* it can be seen that it is always lower than 1.5 except in the upper part of the band at port 2 due to the welding process.

IV. CONCLUSIONS

This paper has presented a broadband antenna to work in the sub 6-GHz frequency band for 3G to 5G standards. The antenna has been designed and fabricated in a cost-effective and affordable way presenting a compact and fully planar topology. The main idea behind the goal is the inclusion of active embedded dipoles in the antipodal part of the antenna itself. Compactness and dual polarized performance have been achieved for working in the whole frequency bandwidth between 1.427 and 2.69 GHz. The performance of the antenna has been shown as good in terms of matching (below −14 dB), isolation (larger than 28 dB), and radiation pattern for a dual-polarization performance of ±45°.

REFERENCES

[1] *Gartner (Symposium/ITxpo 2015, Nov. 8-12th, Barcelona)*.
[2] Y. Wang, J. Li, L. Huang, Y. Jing, A. Georgakopoulos, and P. Demestichas, "5G mobile: Spectrum broadening to higher-frequency bands to support high data rates," *IEEE Veh. Technol. Mag.*, vol. 9, no. 3, pp. 39–46, Sep. 2014.
[3] E. Chavarria-Reyes, I. F. Akyildiz, and E. Fadel, "Energy-efficient multi-stream carrier aggregation for heterogeneous networks in 5G wireless systems," *IEEE Trans. Wireless Commun.*, vol. 15, no. 11, pp. 7432–7443, Nov. 2016.
[4] (Feb. 2020). *Qualcomm: Making 5G NR a Commercial Reality*. [Online]. Available: https://www.qualcomm.com/media/documents/files/making-5g-nr-a-commercial-reality.pdf
[5] Y. Huo, X. Dong, W. Xu, and M. Yuen, "Enabling multi-functional 5G and beyond user equipment: A survey and tutorial," *IEEE Access*, vol. 7, pp. 116975–117008, 2019.
[6] *Technical Specification Group Radio Access Network; NR; User Equipment (UE) Radio Transmission Reception; Part 1: Range 1 Standalone*, document 3GPP TS 38.101-3 V15.3.0, Oct. 2018.
[7] Official Journal of the European Union. (Apr. 26, 2018). *Commission Implementing Decision (EU) 2018/661 of 26 Apr. 2018 Amending Implementing Decision (EU) 2015/750*. [Online]. Available: https://eurlex.europa.eu/eli/dec_impl/2018/661/oj
[8] European Commission. Directorate-General for Communications Networks, Content and Technology. Electronic Communications Networks and Services. Radio Spectrum Policy, Brussels, Belgium. (Mar. 14, 2017). *Mandate to CEPT to Develop Harmonized Technical Conditions in Additional Frequency Bands in the 1.5 GHz Range for Their Use for Terrestrial Wireless Broadband Electronic Communications Services in the Union*. [Online]. Available: http://ec.europa.eu/newsroom/document.cfm?doc_id=45863
[9] Y. Cui, R. Li, and P. Wang, "A novel broadband planar antenna for 2G/3G/LTE base stations," *IEEE Trans. Antennas Propag.*, vol. 61, no. 5, pp. 2767–2774, May 2013.
[10] Y. Cui, R. Li, and P. Wang, "Novel dual-broadband planar antenna and its array for 2G/3G/LTE base stations," *IEEE Trans. Antennas Propag.*, vol. 61, no. 3, pp. 1132–1139, Mar. 2013.
[11] Y. Cui, R. Li, and H. Fu, "A broadband dual-polarized planar antenna for 2G/3G/LTE base stations," *IEEE Trans. Antennas Propag.*, vol. 62, no. 9, pp. 4836–4840, Sep. 2014.
[12] H. Sun, C. Ding, T. S. Bird, and Y. J. Guo, "A base station antenna element with simple structure but excellent performance," in *Proc. Austral. Microw. Symp. (AMS)*, Feb. 2018, pp. 35–36.
[13] N. Xu and Q.-X. Chu, "A broadband dual-polarized antenna with coupling-resonators for base-station applications," in *Proc. Int. Workshop Antenna Technol. (iWAT)*, Mar. 2018, pp. 1–3.
[14] H. Sun, C. Ding, T. Yang, Y. J. Guo, and P. Qin, "A wideband base station antenna with stable radiation pattern," in *Proc. Austral. Microw. Symp. (AMS)*, Feb. 2018, pp. 5–6.
[15] X. Gao, Y. Cui, and R. Li, "Broadband vertically/horizontally dual-polarized antenna for base stations," in *Proc. 11th Int. Symp. Antennas, Propag. EM Theory (ISAPE)*, Oct. 2016, pp. 79–80.
[16] Y. Cui, X. Gao, H. Fu, Q.-X. Chu, and R. Li, "Broadband dual-polarized dual-dipole planar antennas: Analysis, design, and application for base stations," *IEEE Antennas Propag. Mag.*, vol. 59, no. 6, pp. 77–87, Dec. 2017.
[17] D.-L. Wen, D.-Z. Zheng, and Q.-X. Chu, "A dual-polarized planar antenna using four folded dipoles and its array for base stations," *IEEE Trans. Antennas Propag.*, vol. 64, no. 12, pp. 5536–5542, Dec. 2016.
[18] H.-H. Sun, C. Ding, H. Zhu, and Y. J. Guo, "Dual-polarized multi-resonance antennas with broad bandwidths and compact sizes for base station applications," *IEEE Open J. Antennas Propag.*, vol. 1, pp. 11–19, 2020.
[19] M. Li, Q. L. Li, B. Wang, C. F. Zhou, and S. W. Cheung, "A low-profile dual-polarized dipole antenna using wideband AMC reflector," *IEEE Trans. Antennas Propag.*, vol. 66, no. 5, pp. 2610–2615, May 2018.
[20] M. Li, R. Wang, J. M. Yasir, and L. Jiang, "A miniaturized dual-band dual-polarized band-notched slot antenna array with high isolation for base station applications," *IEEE Trans. Antennas Propag.*, vol. 68, no. 2, pp. 795–804, Feb. 2020.
[21] A. Alieldin, Y. Huang, S. J. Boyes, M. Stanley, S. D. Joseph, Q. Hua, and D. Lei, "A triple-band dual-polarized indoor base station antenna for 2G, 3G, 4G and Sub-6 GHz 5G applications," *IEEE Access*, vol. 6, pp. 49209–49216, Sep. 2018.

[22] Q. Zhang and Y. Gao, "A compact broadband dual-polarized antenna array for base stations," *IEEE Antennas Wireless Propag. Lett.*, vol. 17, no. 6, pp. 1073–1076, Jun. 2018.
[23] L. Wu, R. Li, Y. Qin, and Y. Cui, "Bandwidth-enhanced broadband dual-polarized antennas for 2G/3G/4G and IMT services," *IEEE Antennas Wireless Propag. Lett.*, vol. 17, no. 9, pp. 1702–1706, Sep. 2018.
[24] R. C. Hansen and R. E. Collin, *Small Antenna Handbook*. Hoboken, NJ, USA: Wiley, 2011.
[25] S. Martin-Anton and D. Segovia-Vargas, "Dual-polarized broadband antenna for new mobile communication base stations," in *Proc. 13th Eur. Conf. Antennas Propag. (EuCAP)*, Mar./Apr. 2019, pp. 1–3.

SERGIO MARTIN-ANTON was born in Plasencia, Caceres, Spain, in 1992. He received the bachelor's degree in sound and image engineering for telecommunications from Extremadura University, in 2014, obtaining one of the best academic records, and the double master's degree in telecommunications engineering and multimedia and communications from the Universidad Carlos III de Madrid (UC3M), in 2016. He is currently pursuing the Ph.D. degree with the Group of Radiofrequency, Electromagnetics, Microwaves and Antennas (GREMA), Universidad Carlos III de Madrid. In 2014, he was developing his bachelor final project at Kassel University, Germany, with an Erasmus Scholarship, where he learned and experienced with microwave circuits manufacture and measurement. He has authored several national and international congress articles as European Conference on Antennas and Propagation (EUCAP) or International Symposium on Antennas and Propagation and North American Radio Science Meeting (IEEE APS/URSI). His present research interest is focused on base station broadband antennas for new generations of mobile communication systems.

Mr. Martin-Anton's awards and honors also include the Erasmus Scholarship for his German stay and a grant for predoctoral contracts for University Teacher Training (FPU16/00459) by the Spanish Ministry of Education, Culture and Sport.

DANIEL SEGOVIA-VARGAS (Member, IEEE) was born in April 1968. He received the Ph.D. degree *(cum laude)* in telecommunications engineer ETSIT-UPM, in 1998, with a distinction by unanimity. He was a Telecommunications Engineer with ETSIT, UPM, in 1993. From 1993 to 1998, he was an Assistant Professor with the Universidad de Valladolid. Since 1998, he has been a Professor with the Universidad Carlos III de Madrid (UC3M). Since 2001, he has been an Associate Professor (Tenure) of signal theory and communications at the signals with the Universidad Carlos III de Madrid, where he is currently teaching high frequency microwave and circuits and antennas. Since 2003, he has been chairing the Group Radiofrequency, Electromagnetics, Microwaves and Antennas, UC3M. From 2004 to 2010, he was the Head of telecommunications engineering with the Escuela Politécnica Superior, UC3M. Since 2012, he has been the Head of the Escuela Politécnica Superior, Universidad Carlos III de Madrid. He has been a Visiting Researcher with the Rutherford Appleton Laboratory. He has also been a Full Professor with the Universidad Carlos III de Madrid, since 2016. He has authored or coauthored more than 300 publications in scientific journals and international conferences (more than 80 in indexed international journals and more than 20 international invited conferences). His areas of research include antennas (antenna arrays and miniaturized antennas where he is currently leading a project with Airbus on antenna miniaturization for aircraft applications), active antennas, metamaterials and technologies in THz frequencies.

He has been a member of the AP-S Society, since 1998 and the MTT-S Society, since 2001. He received the award from COIT-Ericsson, the best thesis in mobile communication. He was the President and an Organizer of URSI2011, and a member of the Organizing Committee of EuCAP 2010 (where he was the Awards Committee) and on the future EuCAP 2022. He has organized several international Workshops in the domain of metamaterials y technologies of THz. He has been national delegate for European Cost actions in the antennas field (Cost 284, Cost IC0603, and Cost IC1102), since 2002. He has been the Treasurer of the EuMW 2018. He has chaired more than 70 research and development projects, both public and private. He has been the Treasurer of the European Microwave Conference, in 2018.